

Probing topological degeneracy on a torus using superconducting altermagnets

Tsz Fung Heung^{1,2} and Marcel Franz²

¹*Department of Physics, the Hong Kong University of Science and Technology, Clear Water Bay, Hong Kong, China*

²*Department of Physics and Astronomy, and Quantum Matter Institute, University of British Columbia, Vancouver, BC, Canada V6T 1Z1*

(Dated: November 28, 2024)

The notion of topological order (TO) can be defined through the characteristic ground state degeneracy of a system placed on a manifold with non-zero genus g , such as a torus. This ground state degeneracy has served as a key tool for identifying TOs in theoretical calculations but it has never been possible to probe experimentally because fabricating a device in the requisite toroidal geometry is generally not feasible. Here we discuss a practical method that can be used to overcome this difficulty in a class of topologically ordered systems that consist of a TO and its time reversal conjugate $\overline{\text{TO}}$. The key insight is that a system possessing such $\text{TO} \otimes \overline{\text{TO}}$ order fabricated on an annulus behaves effectively as TO on a torus, provided that one supplies a symmetry-breaking perturbation that gaps out the edge modes. We illustrate this general principle using a specific example of a spin-polarized $p_x \pm ip_y$ chiral superconductor which is closely related to the Moore-Read Pfaffian fractional quantum Hall state. Specifically, we introduce a simple model with altermagnetic normal state which, in the presence of an attractive interaction, hosts a helical $(p_x - ip_y)^\uparrow \otimes (p_x + ip_y)^\downarrow$ superconducting ground state. We demonstrate that when placed on an annulus with the appropriate symmetry-breaking edge perturbation this planar two-dimensional system, remarkably, exhibits the same pattern of ground state degeneracy as a $p_x + ip_y$ superconductor on a torus. We discuss broader implications of this behavior and ways it can be tested experimentally.

I. INTRODUCTION

When a 2D system with topological order is placed on a torus (or a surface with higher-genus g), its ground state exhibits a degeneracy that depends on g while the member states of the degenerate ground manifold cannot be distinguished by any local measurement [1–3]. This key feature forms a basis of early proposals to exploit TO systems in fault-tolerant quantum computation. For practical reasons, however, it is generally not possible to prepare 2D quantum systems in the toroidal geometry and hence the ground state degeneracy in its basic form has never been experimentally tested, even for well-established TOs occurring in fractional quantum Hall (FQH) phases. Instead, experimental work to-date [4, 5] has focused on probing either the gapless edge modes in more conventional planar geometries with edges, guaranteed to be present by the bulk-boundary correspondence, or the excitations in the TO bulk, whose fractional charge and exchange statistics [6–9] (possibly non-Abelian) are fundamentally related to the ground state degeneracy on torus [10–13].

For the same reason, attempts to employ TO systems in quantum information storage and processing schemes have focused largely on directly manipulating and probing its non-Abelian anyon excitations [14, 15], often utilizing gapless edge modes in the process. The presence of gapless excitations, however, can make such devices sensitive to noise and decoherence, thus subverting the promise of intrinsic fault tolerance. Clearly, to realize the full potential of fault tolerance inherent to topological orders, it would be preferable to use the ground state degeneracy in a fully gapped TO system for this purpose.

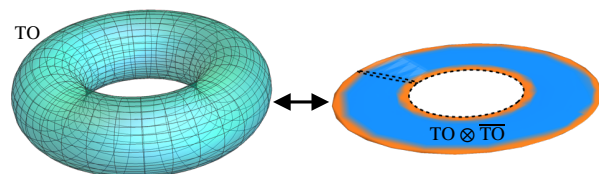


FIG. 1. Equivalence of TO on the torus and $\text{TO} \otimes \overline{\text{TO}}$ on an annulus with edge modes gapped through a symmetry-breaking perturbation, marked here in orange.

Recent work on “Cheshire qudits” [16] advanced a visionary proposal along these lines based on an even-denominator fractional quantum spin Hall (FQSH) state that may be present in twisted homobilayer MoTe_2 according to the recent experimental report [17]. One candidate state consistent with the reported transport signatures is a helical non-Abelian phase composed of a Moore-Read Pfaffian state [18] for spin-up electrons and its time-reversal (\mathcal{T}) conjugate for spin-down electrons [19, 20], or $\text{Pf}^\uparrow \otimes \overline{\text{Pf}}^\downarrow$ for short. This FQSH phase exhibits a pair of gapless helical edge modes protected by a combination of time-reversal, charge conservation and spin/valley symmetries. As noted in Ref. [16], a symmetry-breaking perturbation at the edge can gap out the edge modes. This allows electrons near the edges to tunnel between the Pf^\uparrow and $\overline{\text{Pf}}^\downarrow$ states thus in effect transforming a planar geometry with open edges to a singly connected surface supporting the TO. In this way, a planar flake of twisted homobilayer MoTe_2 with gapped edges can be thought of as having a topology of a sphere with Pf^\uparrow forming its top surface, $\overline{\text{Pf}}^\downarrow$ its bottom surface and the symmetry-breaking perturbation gluing the two halves

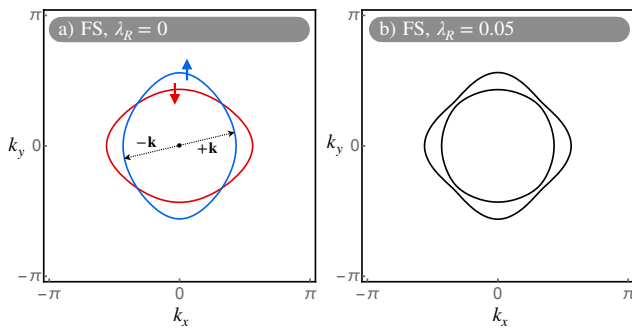


FIG. 2. Spin split Fermi surfaces of the altermagnetic metal described by Hamiltonian Eqs. (1,2) for $\eta = 0.2$ and $\mu = -2.1$, with (b) and without (a) Rashba SOC.

together. Similarly, a flake with a hole punched through its middle can be thought of as a torus pictured in Fig. 1.

In Ref. [16] this equivalence was argued at the level of topological field theory. The purpose of this work is to perform a study in the framework of a microscopic model which can offer a complementary and potentially deeper understanding of the physics that is involved. To this end we employ the well-known equivalence between the Moore-Read Pfaffian state and the weak-pairing state of fermions realizing a spin-polarized $p_x \pm ip_y$ superconductor, or p_{\pm} for short. According to Read and Green [21] the many-body wavefunctions of the two systems are asymptotically the same. As a result, they also share many key physical properties, including the edge states, quasihole exchange statistics and toroidal ground state degeneracy.

To simulate a toroidal geometry using the equivalence principle depicted in Fig. 1 we construct a simple model of 2D electrons whose ground state in the presence of a weak attractive interaction can be described as a helical $(p_x - ip_y)^{\uparrow} \otimes (p_x + ip_y)^{\downarrow}$ superconductor, abbreviated in the following as $p_{-}^{\uparrow} \otimes p_{+}^{\downarrow}$. The construction is based on a normal state that can be characterized as an altermagnetic metal [22–25] with a pair of spin-split Fermi surfaces related by a C_4 rotation and time reversal \mathcal{T} , pictured in Fig. 2(a). The key observation is that such a spin-split Fermi surface cannot support the conventional spin singlet pairing; instead the leading instability is toward an odd-parity, \mathcal{T} broken $p_x \pm ip_y$ chiral phase in each spin channel. We emphasize that this unconventional pairing state does not require any exotic microscopic mechanism or unusual form of the attractive interaction; instead it is a generic property of the spin-split Fermi surface characteristic of an altermagnet and will form through the conventional BCS mechanism in the presence of e.g. phonon-mediated attraction.

Furthermore, we show that a weak Rashba spin-orbit coupling (SOC), acting either in the bulk or near the edges, selects a state with opposite chiralities for two spin species and hence stabilizes the $p_{-}^{\uparrow} \otimes p_{+}^{\downarrow}$ helical phase.

Intrinsic or proximity-generated spin-singlet SC order at the edge has the same effect. Importantly, these same perturbations also gap out the helical edge modes that would otherwise exist in the pure $p_{-}^{\uparrow} \otimes p_{+}^{\downarrow}$ phase. Hence, we argue that such a simple minimal model possesses all the ingredients that are necessary to test the annulus/torus correspondence. Also, since several metallic altermagnet candidate materials have recently been experimentally confirmed [26–30], altermagnets with SC order may offer a platform to probe the topological degeneracy in a simple setting, in addition to providing insights into the physics of the helical Moore-Read Pfaffian state that may be present in twisted homobilayer MoTe_2 .

A BCS-type Hamiltonian describing superconducting states conserves electron number parity but not the electron number itself. Accordingly, the eigenstates of such Hamiltonians can be classified as parity even and parity odd. The chiral $p_x + ip_y$ superconductor exhibits four-fold ground state degeneracy when placed on a torus. Importantly, three of those states belong to the even parity sector and one to the odd parity sector [21]. This subtle feature is deeply rooted in the non-Abelian exchange statistics of vortices in the chiral p -wave state [31] and distinguishes it from an ordinary s -wave superconductor [12, 13]. When placed on a torus, the latter also exhibits four-fold ground-state degeneracy [32] but in this case all four ground states belong to the even parity sector. In the following we shall review the origin of this ground state degeneracy and its robustness against disorder. We then demonstrate the even/odd parity effect in the ground state manifold of the chiral p_{\pm} state on the torus and the helical $p_{-}^{\uparrow} \otimes p_{+}^{\downarrow}$ on an annulus with gapped boundaries, thus establishing their equivalence. In closing we discuss broader significance of these results and ways these effects can be probed experimentally.

II. MICROSCOPIC MODEL

A. Altermagnetic normal metal

As the starting point we consider a minimal model of a ‘ d -wave’ altermagnetic metal [23, 24] in two dimensions defined by the Hamiltonian $\mathcal{H}_0 = \sum_{\mathbf{k}} \psi_{\mathbf{k}}^{\dagger} h_0(\mathbf{k}) \psi_{\mathbf{k}}$ with $\psi_{\mathbf{k}} = (c_{\mathbf{k}\uparrow}, c_{\mathbf{k}\downarrow})^T$ and

$$h_0(\mathbf{k}) = -2t(\cos k_x + \cos k_y) - 2\eta\sigma_z(\cos k_x - \cos k_y). \quad (1)$$

Here σ_{μ} are Pauli matrices in spin space, t denotes the nearest neighbor hopping amplitude on the square lattice and η controls the altermagnetic band splitting. The latter breaks time-reversal symmetry \mathcal{T} but the model remains invariant under combined C_4 rotation and \mathcal{T} , a hallmark feature of altermagnets which guarantees vanishing total magnetization. The spin-split Fermi surfaces following from Eq. (1) are depicted in Fig. 2(a). This type of non-relativistic spin splitting has recently been experimentally observed in MnTe [27, 28], RuO_2 [29] and

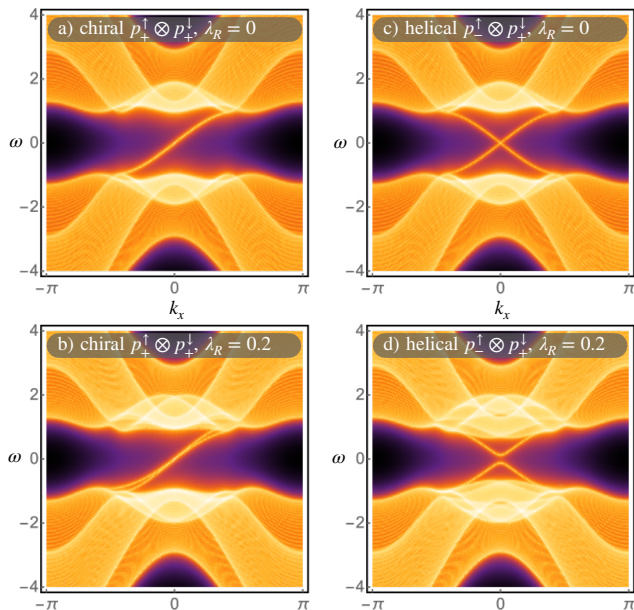


FIG. 3. Edge states in chiral and helical phases. Spectral function $A_y(\omega, k_x) = -2\text{Im}[\omega + i\delta - H(k_x)]_{yy}^{-1}$ for the superconducting system Eq. (3) placed on a long strip with open boundaries in the y -direction (width 52 sites) and periodic boundary conditions along x . The spectral function is averaged over the lower half of the strip (sites 1-26) to clearly show the spectrum associated with one edge. Note that there are two distinct edge modes in the chiral $p_+^\uparrow \otimes p_+^\downarrow$ phase shown in panel (c), consistent with $C = 2$. They become more clearly visible in panel (d) where the degeneracy is lifted by SOC. We use $\eta = 0.2$, $\mu = -2.1$, $\Delta_\sigma = 0.5$ and λ_R as indicated.

CrSb thin films [30]. In addition, recent theoretical work [33–38] identified several families of other materials as candidate altermagnets.

When placed on a substrate the inversion symmetry of \mathcal{H}_0 will generically be broken and a Rashba SOC term

$$h_R(\mathbf{k}) = 2\lambda_R(\sigma_x \sin k_y - \sigma_y \sin k_x) \quad (2)$$

becomes symmetry-allowed. For λ_R non-zero Fermi crossings along the Brillouin zone diagonals are split, Fig. 2(b) as the Rashba term causes the spins to rotate into the plane in their vicinity. In the following, we will consider superconducting instabilities of \mathcal{H}_0 , and, when specified assume weak SOC with magnitude small compared to the SC gap. We will take $t = 1$ and express all energies in units of t .

B. Paired state

It is clear that for weak attractive interactions the type of FS depicted in Fig. 2(a) cannot support the conventional spin-singlet SC state with zero-momentum Cooper pairs. Except for the 4 points where the two Fermi surfaces intersect, to form a zero-momentum Cooper pair an electron with crystal momentum $+\mathbf{k}$ must pair with

the *same spin* electron at momentum $-\mathbf{k}$. Such an equal-spin pairing requires an orbital pair wave-function that is odd under inversion. On the square lattice the simplest possibility is the p -wave state. Furthermore, to maximize the condensation energy the paired state should be fully gapped which leads directly to the chiral p_\pm pair state in each spin channel as the most natural SC ground state compatible with the altermagnetic normal metal Eq. (1). This conclusion is consistent with the results of Ref. [39] where a similar model was solved self-consistently and with our own computations [40].

The SC state can be described using a four-component Nambu spinor $\Psi_{\mathbf{k}} = (c_{\mathbf{k}\uparrow}, c_{\mathbf{k}\downarrow}, c_{-\mathbf{k}\uparrow}^\dagger, -c_{-\mathbf{k}\downarrow}^\dagger)^T$ and the Bogoliubov-de Gennes (BdG) Hamiltonian of the form

$$\mathcal{H} = \sum_{\mathbf{k}} \Psi_{\mathbf{k}}^\dagger \begin{pmatrix} h_{\mathbf{k}} & \hat{\Delta}_{\mathbf{k}} \\ \hat{\Delta}_{\mathbf{k}}^\dagger & -h_{\mathbf{k}}^* \end{pmatrix} \Psi_{\mathbf{k}}, \quad (3)$$

with $h_{\mathbf{k}} = h_0(\mathbf{k}) + h_R(\mathbf{k}) - \mu$ and the pair field matrix $\hat{\Delta}_{\mathbf{k}} = \text{diag}(\Delta_{\mathbf{k}\uparrow}, \Delta_{\mathbf{k}\downarrow})$. Here

$$\Delta_{\mathbf{k}\sigma} = \Delta_\sigma(\sin k_x \pm i \sin k_y) \quad (4)$$

are chiral p -wave order parameters for spin σ electrons and μ denotes the chemical potential.

In the absence of SOC the two spin channels are uncoupled and the 4×4 BdG matrix in Eq. (3) becomes block-diagonal in spin space. Each block then describes an independent $p_x \pm ip_y$ superconductor for a given spin projection, with a fully gapped excitation spectrum

$$E_{\mathbf{k}\sigma} = \sqrt{(\epsilon_{\mathbf{k}\sigma} - \mu)^2 + |\Delta_{\mathbf{k}\sigma}|^2}, \quad (5)$$

where $\epsilon_{\mathbf{k}\sigma}$ denote the normal-state excitation energies of spin- σ electrons that follow from Eq. (1). Viewed in isolation each such superconductor is topological, characterized by a nonzero BdG Chern number $C = \pm 1$ for $p_x \pm ip_y$, respectively. Of the 4 degenerate ground states of the combined spin up/down sectors two are chiral, namely $p_+^\uparrow \otimes p_+^\downarrow$ and $p_-^\uparrow \otimes p_-^\downarrow$, with the total Chern number $C = +2$ and -2 , respectively. The remaining two are helical and have $C = 0$. Correspondingly, when placed on a long strip their excitation spectra exhibit chiral or helical gapless edge modes shown in Fig. 3(a,c). Note that the 4-fold degeneracy mentioned above simply refers to 4 possible combinations of $+/-$ signs in Eq. (4) and is unrelated to the topological degeneracy on a torus that we discuss below.

The presence of SOC ($\lambda_R \neq 0$) alters the above picture in two important ways. First, in the absence of inversion symmetry one can no longer classify pairing as even or odd under inversion. Instead, the two channels can mix. For weak Rashba SOC we thus expect the pair field matrix $\hat{\Delta}$ to acquire small off-diagonal elements that represent spin-singlet components of the SC order parameter allowed by symmetry. Second, the Rashba term couples spin up and down sectors of the BdG Hamiltonian Eq. (3). This has the effect of splitting the four-fold ground

state degeneracy mentioned above. We find, consistent with the results of Ref. [39], that Rashba SOC favors one of the helical states with total Chern number $C = 0$, specifically $p_-^\uparrow \otimes p_+^\downarrow$. Intuitively, this can be understood as follows. Microscopically, the Rashba term originates from the atomic SOC term $\mathbf{S} \cdot \mathbf{L}$ which conserves the total angular momentum $\mathbf{J} = \mathbf{S} + \mathbf{L}$. It is easy to see that $p_-^\uparrow \otimes p_+^\downarrow$ is compatible with this conservation law while the other three states are not. Specifically, J_z of both components in $p_-^\uparrow \otimes p_+^\downarrow$ vanishes (for instance a p_-^\uparrow Cooper pair has $s_z = 2 \times (1/2)$ and $l_z = -1$) and hence Rashba induced transfer of a Cooper pair from p_-^\uparrow to p_+^\downarrow conserves the total angular momentum \mathbf{J} .

According to the above discussion in the presence of a small but nonzero λ_R , our system has a unique ground state characterized as $p_-^\uparrow \otimes p_+^\downarrow$. A detailed calculation supporting this conclusion is presented in Appendix A, where we also discuss the effect of proximity induced spin singlet pairing and applied in-plane magnetic field B_x . The former also gaps out the helical edge modes but, in contrast to SOC, admits two degenerate ground states, namely $p_-^\uparrow \otimes p_+^\downarrow$ and $p_+^\uparrow \otimes p_-^\downarrow$. Zeeman field, on the other hand, is found to select the two chiral phases as ground states. We thus conclude that by applying perturbations listed above one can efficiently control the system and select any of the four degenerate ground states, making the SC altermagnet a flexible and potentially useful platform for explorations of topological superconductivity.

We finally note an important case of spontaneously generated SC gap at the edge of the helical phase in the absence of any perturbation ($\lambda_R = B_x = 0$) or proximity effect. Because the edge breaks the inversion symmetry one expects pairing near the edge to mix p and s channels and hence permit opposite-spin pairing, even if the bulk is purely equal-spin p -wave. Indeed the two helical edge modes displayed in Fig. 3(c) belong to the opposite spin projections \uparrow and \downarrow . In the presence of attractive interactions (e.g. those responsible for the bulk p -wave SC order) these low-energy modes will be susceptible to the formation of Cooper pairs composed of the time-reversed edge states $(+k, \uparrow)$ and $(-k, \downarrow)$. The corresponding term in the BdG Hamiltonian will be

$$\delta\mathcal{H} = \sum_{k,y} \left[\Delta_k^{\text{edge}}(y) c_{k\uparrow}^\dagger(y) c_{-k\downarrow}^\dagger(y) + \text{h.c.} \right] \quad (6)$$

with k denoting the momentum along the edge and y the perpendicular coordinate. As we will demonstrate below, non-zero $\Delta_k^{\text{edge}}(y)$ opens a gap in the helical modes. Importantly, it also facilitates coupling between spin-up and spin-down sectors of the theory, hence enabling the torus/annulus correspondence indicated in Fig. 1.

Edge modes in the two chiral phases are protected by the bulk topological invariant and hence cannot be gapped by any perturbation that does not close the bulk gap. For this reason we expect the two helical phases with gapped edges (due to Δ^{edge}) to be energetically favored over the chiral phases even in the absence of any

other symmetry breaking perturbations, such as SOC.

C. Symmetries

The BdG Hamiltonian in Eq. (3) respects the charge conjugation symmetry \mathcal{C} generated by $\sigma_z \tau_x H_{-\mathbf{k}}^* \tau_x \sigma_z = -H_{\mathbf{k}}$ with $\mathcal{C}^2 = +1$. Here $H_{\mathbf{k}}$ refers to the 4×4 BdG matrix in Eq. (3) and τ are Pauli matrices in the Nambu space. This places the system in the Altland-Zirnbauer class D which has an integer topological classification in two dimensions; the relevant index is just the BdG Chern number mentioned above which is indeed non-zero for the two chiral ground states.

In the absence of SOC the two helical states respect an additional antiunitary symmetry $\mathcal{T}' = C_4 \mathcal{T}$ with $\mathcal{T}'^2 = -1$. The system is then in class DIII which has \mathbb{Z}_2 topological classification in two dimensions. However, because the edge breaks the C_4 rotation symmetry the corresponding \mathbb{Z}_2 index alone cannot protect the Kramers-like degeneracy between the two edge modes at $k = 0$, clearly visible in Fig. 3(c). The edge mode crossing is instead protected by the $\mathbb{Z}_2^\uparrow \times \mathbb{Z}_2^\downarrow$ number parity conservation symmetry that is a remnant of the $U(1)^\uparrow \times U(1)^\downarrow$ electron number conservation present in the normal state.

Simply put, as long as the two spin blocks remain decoupled the crossing of the two helical edge modes will be protected. Any perturbation that couples the two spin sectors breaks the $\mathbb{Z}_2^\uparrow \times \mathbb{Z}_2^\downarrow$ symmetry down to a single \mathbb{Z}_2 associated with the global number parity conservation and will generically open a gap.

Indeed we see in Fig. 3(d) that $\lambda_R \neq 0$ opens up a gap in the edge modes at $k = 0$. Adding a small spin-singlet component to the SC pair matrix likewise couples the two spin projections, breaks the $\mathbb{Z}_2^\uparrow \times \mathbb{Z}_2^\downarrow$ symmetry by the same mechanism and gaps out the helical edge modes. Applied in-plane magnetic field that acts as a Zeeman term $\mathbf{B}_\parallel \cdot \boldsymbol{\sigma}$ also breaks the symmetry and opens a gap if \mathbf{B}_\parallel has a non-zero projection onto the edge (otherwise a mirror symmetry protects the helical crossing).

III. TOPOLOGICAL DEGENERACY ON TORUS

In this Section we summarize the known facts about topological degeneracy of superconductors. We review both conventional spin-singlet s -wave and equal-spin chiral p -wave cases. According to the modern theory [32] both are characterized by topological order when placed on a torus with a subtle difference distinguishing s - and p -wave paired states, closely related to the non-Abelian exchange statistics of vortices in the latter [12]. This is one of the key properties that chiral p -wave SC shares with the Moore-Read Pfaffian fractional quantum Hall state [13, 21].

A. General considerations

According to the modern understanding superconductors are topologically ordered phases of matter [32]. The ground-state degeneracy is associated with the even/odd number of superconducting magnetic flux quanta $\Phi_0 = hc/2e$ threaded through the two holes of the torus. To illustrate this in the simplest possible setting we consider weak-coupling continuum BCS theory defined by the BdG Hamiltonian of the form

$$\mathcal{H} = \sum_{\mathbf{k}} \Psi_{\mathbf{k}}^\dagger \begin{pmatrix} \xi_{\mathbf{k}} & \Delta_{\mathbf{k}} \\ \Delta_{\mathbf{k}}^* & -\xi_{\mathbf{k}} \end{pmatrix} \Psi_{\mathbf{k}}, \quad (7)$$

where $\xi_{\mathbf{k}} = \hbar^2 k^2/2m - \mu$ is the kinetic energy referenced to the chemical potential μ . For spin-singlet s -wave we have

$$\Delta_{\mathbf{k}} = \Delta_s, \quad \Psi_{\mathbf{k}} = \begin{pmatrix} c_{\mathbf{k}\uparrow} \\ c_{-\mathbf{k}\downarrow}^\dagger \end{pmatrix}, \quad (8)$$

while for equal-spin chiral p -wave

$$\Delta_{\mathbf{k}} = \Delta_p(k_x - ik_y), \quad \Psi_{\mathbf{k}} = \begin{pmatrix} c_{\mathbf{k}} \\ c_{-\mathbf{k}}^\dagger \end{pmatrix}. \quad (9)$$

The toroidal geometry is implemented by imposing periodic boundary conditions along both x and y directions which, for a system of size $L_x \times L_y$, implies discrete values for the allowed momenta

$$\mathbf{k} = 2\pi(n_x/L_x, n_y/L_y), \quad n_x, n_y \in \mathbb{Z}. \quad (10)$$

Magnetic fluxes (Φ_x, Φ_y) threaded through the torus holes are included by the minimal substitution in the kinetic term, $\mathbf{k} \rightarrow -i\nabla - (e/\hbar c)\mathbf{A}$ where \mathbf{A} is the vector potential satisfying

$$\oint_{\Omega_j} \mathbf{A} \cdot d\mathbf{l} = \Phi_j, \quad (11)$$

with Ω_j denoting a non-contractible loop on the torus. We will work in the gauge $\mathbf{A} = (\Phi_x/L_x, \Phi_y/L_y)$ which preserves the translational invariance of the original problem.

When the magnetic flux is non-zero the superconductor will carry persistent current with density

$$\mathbf{j}_s = \rho_s \left(\nabla\varphi - \frac{2e}{\hbar c}\mathbf{A} \right), \quad (12)$$

where ρ_s denotes the superfluid density. Such a current incurs an energy cost $\propto \mathbf{j}_s^2$ per unit area. In Eq. (12) φ denotes the phase of the pair field $\Delta_s(\mathbf{r}) = \Delta_0 e^{i\varphi(\mathbf{r})}$ which is allowed to vary along the torus so as to minimize the system energy. Importantly, such spatial variations are constrained by single-valuedness of $\Delta_s(\mathbf{r})$ which implies that $\varphi(\mathbf{r})$ can wind by an integer multiple of 2π along each non-contractible loop. For p -wave it is necessary to symmetrize the placement of the phase,

$\Delta_p(\mathbf{r}) = \Delta_0 e^{i\varphi(\mathbf{r})/2} (-i\partial_x + \partial_y) e^{i\varphi(\mathbf{r})/2}$, in order to ensure full gauge invariance of the theory [41, 42].

A non-zero phase winding can be thought of as inserting a vortex into one of the torus holes. Mathematically, we can describe it as

$$\varphi(\mathbf{r}) = 2\pi\mathbf{r} \cdot (m_x/L_x, m_y/L_y) \quad (13)$$

where integers (m_x, m_y) count vortices in two holes. A vortex will enter when it lowers the system ground state energy. If we slowly ramp up the flux Φ_x from zero the increasing supercurrent will drive the energy up in proportion to \mathbf{j}_s^2 . When Φ_x exceeds $\Phi_0/2$ Fig. 4(a) shows that it becomes energetically favorable to insert a vortex and partially screen the supercurrent. At $\Phi_x = \Phi_0$ this screening becomes complete and no current flows once again by virtue of the perfect cancellation of the vector potential term in Eq. (12) by $\nabla\varphi$.

It is useful to bring the BdG Hamiltonian in the presence of vortices back into translation-invariant form. This is achieved by a ‘‘large’’ gauge transformation on the electron operators

$$\Psi_{\mathbf{r}} = \begin{pmatrix} c_{\mathbf{r}\uparrow} \\ c_{\mathbf{r}\downarrow}^\dagger \end{pmatrix} \rightarrow \begin{pmatrix} e^{i\varphi(\mathbf{r})} c_{\mathbf{r}\uparrow} \\ c_{\mathbf{r}\downarrow}^\dagger \end{pmatrix}. \quad (14)$$

and similar for p -wave. In this representation the Hamiltonian Eq. (7) can be written in momentum space as

$$H_{\mathbf{k}} = \begin{pmatrix} \xi_{\mathbf{k}-\mathbf{a}+2\mathbf{v}} & \Delta_{\mathbf{k}+\mathbf{v}} \\ \Delta_{\mathbf{k}+\mathbf{v}} & -\xi_{\mathbf{k}+\mathbf{a}} \end{pmatrix}, \quad (15)$$

where we defined

$$\begin{aligned} \mathbf{a} &= (e/\hbar c)\mathbf{A} = \pi(\Phi_x/L_x, \Phi_y/L_y)/\Phi_0, \\ \mathbf{v} &= \frac{1}{2}\nabla\varphi = \pi(m_x/L_x, m_y/L_y), \end{aligned} \quad (16)$$

and both $\xi_{\mathbf{k}}$ and $\Delta_{\mathbf{k}}$ are now real. Note that Eq. (15) is valid for both s - and p -wave order parameters

In the special case when the magnetic flux is an integer multiple of Φ_0 and matches the number of vortices, that is when

$$(\Phi_x, \Phi_y) = \Phi_0(m_x, m_y), \quad (17)$$

we have $\mathbf{a} = \mathbf{v} = \pi(m_x/L_x, m_y/L_y)$ and the Hamiltonian Eq. (15) becomes

$$H_{\mathbf{k}} = \begin{pmatrix} \xi_{\mathbf{k}+\mathbf{v}} & \Delta_{\mathbf{k}+\mathbf{v}} \\ \Delta_{\mathbf{k}+\mathbf{v}} & -\xi_{\mathbf{k}+\mathbf{v}} \end{pmatrix}. \quad (18)$$

We observe that insertion of magnetic fluxes that satisfy Eq. (17), leads to a simple shift of momenta $\mathbf{k} \rightarrow \mathbf{k} + \mathbf{v}$ in the original zero-flux Hamiltonian Eq. (7). For a large system this explains why all such states are degenerate in energy. Fundamentally, this is nothing but the well-known statement of flux-quantization: superconductor is able to screen the external magnetic field threaded through a hole by adjusting its phase as long the flux is an integer multiple of the SC flux quantum Φ_0 .

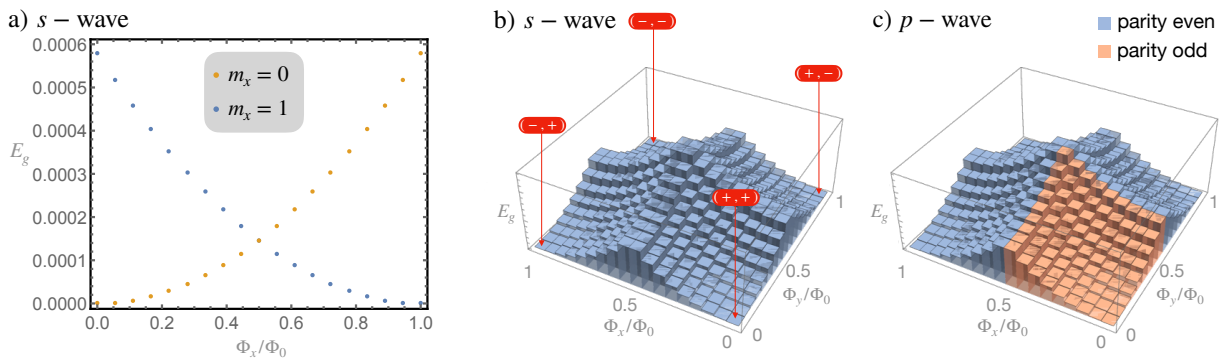


FIG. 4. Ground state energy E_g of (a-b) s -wave and (c) weak-pairing chiral p -wave superconductor on a torus as a function of magnetic fluxes Φ_x and Φ_y threaded through its holes. We use the lattice model with $t = 1$, $\mu = -2.1$ and $\Delta_0 = 0.1$. The results are insensitive to exact values, except for parity in (b) which requires $-4 < \mu < +4$ to remain in the weak-pairing phase.

There is, however, an important distinction between even and odd number of SC flux quanta threading the torus which lies at the root of the topological degeneracy. For even m_j the new allowed values of momenta are simply shifted by one unit and continue to satisfy Eq. (10) with n_j integral. Hence, the electron wavefunctions are identical to those in the absence of flux. For odd m_j , however, the momenta are shifted by *half a unit*, meaning that the Hamiltonian is now equivalent to Eq. (7) with one or both of n_j in Eq. (10) half-integral. In real space this corresponds to antiperiodic boundary conditions for the wavefunctions which are therefore distinct from the zero flux case. This gives rise to four ground states that we label by a pair of indices

$$(\nu_x, \nu_y) = ((-1)^{m_x}, (-1)^{m_y}), \quad (19)$$

with distinct and mutually orthogonal many-body wavefunctions.

As already mentioned, in the thermodynamic limit the four ground states become asymptotically degenerate because the total energy in a large system is not expected to depend on periodic versus antiperiodic boundary conditions. The degeneracy is topological in the sense that no local measurement made within the 2D system can distinguish between the ground states; to detect the fluxes one must perform non-local measurements along two non-contractible loops of the torus.

B. s -wave state

To illustrate the above general considerations we calculate the ground state energy of an s -wave superconductor placed on a torus in the presence of arbitrary fluxes (Φ_x, Φ_y) . This is obtained by summing all negative eigenvalues of the BdG Hamiltonian Eq. (15) and minimizing the result over the number of inserted vortices. For the numerical evaluation it is easier to revert to the lattice model with $\xi_{\mathbf{k}} = -2t(\cos k_x + \cos k_y) - \mu$. The result of this computation is given in Fig. 4(a) and clearly shows

minima at integer fluxes corresponding to four degenerate ground states labeled in accord with Eq. (19) as $(+, +)$, $(+, -)$, $(-, +)$ and $(-, -)$.

C. Chiral p -wave state

The analysis for chiral p -wave proceeds along the same path and leads to the same conclusion of four-fold ground state degeneracy on a torus. There is, however, one important difference: Whereas in the s -wave SC all four degenerate ground states belong to the even parity subspace, for chiral p -wave in the weak pairing phase one of the ground states, namely $(+, +)$, belongs to the odd-parity subspace [21]. As we shall see this subtle distinction is fundamentally related to the non-Abelian exchange statistics of vortices in the chiral p -wave phase.

To understand the significance of the above statement recall that while BdG Hamiltonians do not conserve electron number they do conserve the number parity. Hence any eigenstate can be classified as parity even or parity odd. The BCS many-body ground state (for the p -wave case) can be written as

$$|\Psi_G\rangle = \prod_{\mathbf{k}}' (u_{\mathbf{k}} + v_{\mathbf{k}} c_{\mathbf{k}}^\dagger c_{-\mathbf{k}}^\dagger) |0\rangle, \quad (20)$$

where the prime indicates that each pair is to be included once. $(u_{\mathbf{k}}, v_{\mathbf{k}})$ denote the BCS coherence factors which satisfy

$$|u_{\mathbf{k}}|^2 = \frac{1}{2} \left(1 + \frac{\xi_{\mathbf{k}}}{E_{\mathbf{k}}} \right), \quad |v_{\mathbf{k}}|^2 = \frac{1}{2} \left(1 - \frac{\xi_{\mathbf{k}}}{E_{\mathbf{k}}} \right), \quad (21)$$

with $E_{\mathbf{k}} = \sqrt{\xi_{\mathbf{k}}^2 + |\Delta_{\mathbf{k}}|^2}$ and $u_{\mathbf{k}}/v_{\mathbf{k}} = -(E_{\mathbf{k}} - \xi_{\mathbf{k}})/\Delta_{\mathbf{k}}^*$.

In the $(+, +)$ sector the product in Eq. (20) includes the $\mathbf{k} = 0$ term. (The other three sectors obey antiperiodic boundary condition in at least one direction which implies that the $\mathbf{k} = 0$ term is absent from the product.) Importantly, $\Delta_{\mathbf{k}}$ vanishes at $\mathbf{k} = 0$ which according to Eq. (21) implies that the corresponding coherence factor

v_0 also vanishes. This is a manifestation of the simple fact that under equal-spin pairing there is only a single electron state available at $\mathbf{k} = 0$ and one therefore cannot form a Cooper pair from electrons at $+\mathbf{k}$ and $-\mathbf{k}$. Instead, one must consider the occupancy of this state separately. The single state at $\mathbf{k} = 0$ will be occupied provided $\mu > 0$ which defines the weak-pairing phase of the model [21]. The ground-state wave-function in the weak-pairing phase hence reads

$$|\Psi_G^{(+,+)}\rangle = \prod_{\mathbf{k}}' (u_{\mathbf{k}} + v_{\mathbf{k}} c_{\mathbf{k}}^{\dagger} c_{-\mathbf{k}}^{\dagger}) c_0^{\dagger} |0\rangle, \quad (22)$$

and belongs to the odd parity subspace of the theory. The other three ground states, namely $(-, +)$, $(+, -)$ and $(-, -)$, are described by Eq. (20) and belong to the even parity subspace. In the following we will refer to this feature as the “3:1 parity rule”.

In the strong pairing phase ($\mu < 0$) all four sectors are described by Eq. (20) and belong to the even parity subspace. Ground states of a spin-singlet s -wave SC discussed in the previous subsection likewise belong to the even parity subspace.

Fig. 4(b) shows the ground state energy, calculated for the lattice model with the pair field given by Eq. (4). As for s -wave we observe four degenerate ground states at integer fluxes. However, this being a weak-pairing chiral p -wave phase, we now have an odd-parity ground state in the quadrant containing the $(+, +)$ absolute minimum.

The discussion given above may give an impression that the 3:1 parity rule of the ground state manifold in the weak pairing phase of a $p_x + ip_y$ superconductor is a fragile property because it relies e.g. on the perfect translation invariance that allows a description in terms of the crystal momentum. However, this is not the case. The 3:1 rule is a robust topological property of the weak pairing phase and persists in the presence of disorder and other perturbations that do not close the gap between the ground state manifold and the excited states. This can be established by an adiabatic continuity argument and also, perhaps more instructively, by appealing to the Oshikawa-Senthil construction [12, 13] which, based on earlier works [10, 11], establishes a fundamental relation between the ground state degeneracy on a torus and the existence of fractionalized excitations. Specifically, this powerful argument shows that one can cycle between the individual ground states by creating a pair of such fractional excitations, dragging one of them along a non-contractible loop and then again annihilating the pair.

Applied to the problem at hand the 3:1 property can be understood as a fundamental consequence of the non-Abelian nature of vortex/antivortex excitations in the weak pairing phase of a chiral p -wave superconductor and mirrors that of the Moore-Read fractional quantum Hall phase. It turns out that, if one attempts to create the $(+, +)$ state starting from any of the even-parity ground states, the above procedure instead leads to an excited state with an extra Bogoliubov quasiparticle above the

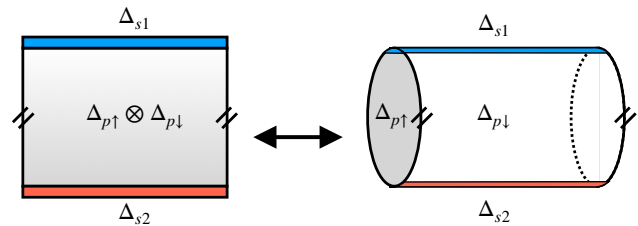


FIG. 5. $p_{-}^{\uparrow} \otimes p_{+}^{\downarrow}$ state on a strip with spin-singlet SC order spontaneously nucleated near its horizontal edges (left) is electronically equivalent to chiral p -wave on a cylinder (right). With periodic boundary conditions along x this has a topology of a torus.

$(+, +)$ ground state. Removing this quasiparticle then gives the odd-parity ground state adiabatically connected to Eq. (22). This conclusion is general and does not require translation-invariant system. In the next Section we shall demonstrate that both the ground-state degeneracy and the 3:1 parity effect characteristic of the weak-pairing phase occur in the model introduced in Sec. II when placed on an annulus and persist in the presence of disorder.

IV. TOPOLOGICAL DEGENERACY ON ANNULUS

We now consider the $p_{-}^{\uparrow} \otimes p_{+}^{\downarrow}$ phase of the model introduced in Sec. II and show that, when placed on an annulus with the appropriate symmetry breaking edge perturbations, it exhibits the ground-state degeneracy characteristic of the chiral p -wave superconductor on a torus. For reasons that will become clear momentarily we consider a very weak uniform Rashba SOC to stabilize the helical $p_{-}^{\uparrow} \otimes p_{+}^{\downarrow}$ phase, and include a spontaneously generated s -wave order parameter near the edges to play the role of the symmetry breaking edge perturbation.

A. Long strip geometry

As a warm-up exercise we first place the $p_{-}^{\uparrow} \otimes p_{+}^{\downarrow}$ superconductor on a long strip with periodic boundary conditions (b.c.) along x and open along y , illustrated in Fig. 5. According to our discussion in Sec. I, when equipped with symmetry breaking perturbations along the open edges, this configuration can be thought of as having a topology of the torus. The two spin sectors, decoupled in the bulk of the strip, furnish the opposite walls of the torus while the symmetry breaking perturbations along the edges serve to glue the two walls together by allowing electrons to flip their spin and hence circle around the full cycle. While this configuration may not be easy to realize in the laboratory (due to periodic boundary conditions along x) it is instructive to consider theoretically because of its translation invariance in one direction. In the next

TABLE I. Parity P and ground state energy splitting parameter $\varepsilon^{(\nu_x, \nu_y)}$ for the four ground state sectors in the long strip geometry. $N_x = 64$ in all cases while N_y varies as indicated. We use $\eta = 0.2$, $\mu = -2.1$, $\Delta_{p\sigma} = 0.5$, $\Delta_{sj} = \pm 0.2$ and $\lambda_R = 0$.

(ν_x, ν_y)	(+, +)	(+, -)	(-, +)	(-, -)
P	+	-	+	+
$\varepsilon (N_y = 16)$	-5.15163×10^{-10}	-3.93501×10^{-10}	3.93491×10^{-10}	5.15174×10^{-10}
$\varepsilon (N_y = 32)$	-2.26019×10^{-10}	-2.26019×10^{-10}	2.26019×10^{-10}	2.26019×10^{-10}
$\varepsilon (N_y = 64)$	-1.12745×10^{-10}	-1.12745×10^{-10}	1.12745×10^{-10}	1.12745×10^{-10}

subsection we will consider a true annulus which can be easily fabricated and shows identical behavior.

To model this geometry we adapt Hamiltonian Eq. (3) by partially Fourier transforming to real space along y and add the edge term Eq. (6) to facilitate transfer of electrons between the spin sectors. For simplicity we assume Δ_k^{edge} to be real, k -independent and equal to $\Delta_{s1,2}$ as indicated in Fig. 5. This choice can be understood by considering the corresponding Ginzburg-Landau free energy, which in the absence of SOC contains, to the lowest order, the following terms coupling edge order parameters to the bulk,

$$-\beta_{sp} \sum_{j=1,2} (\Delta_{sj}^2 \Delta_{p\uparrow}^* \Delta_{p\downarrow}^* + \text{c.c.}), \quad (23)$$

with β_{sp} a positive constant. Bilinear terms, such as $\Delta_{sj} \Delta_{p\uparrow}^*$, are not allowed because they are odd under $x \rightarrow -x$ in the geometry under consideration. Note that adding weak SOC breaks this symmetry and we will discuss this effect separately.

Eq. (23) reveals an important sign ambiguity: switching $\Delta_{sj} \rightarrow -\Delta_{sj}$ has no effect on the GL free energy. In addition, Eq. (23) implies that we can always choose Δ_{sj} to be real if we also choose $\Delta_{p\uparrow} \Delta_{p\downarrow}$ as real. This follows from inspecting the corresponding Josephson energy, proportional to $-\cos(2\varphi_{sj} - \varphi_{p\uparrow} - \varphi_{p\downarrow})$ where φ denote various order parameter phases. The Josephson energy is minimized by taking $\varphi_{p\uparrow} = -\varphi_{p\downarrow}$ and $\varphi_{sj} = 0, \pi$. We will see below that while individual signs of Δ_{sj} are arbitrary, the sum of their phases $\varphi_{s1} + \varphi_{s2}$ has physical significance; it plays the role of the Aharonov-Bohm-like phase of an electron traversing the y -cycle of the torus.

Periodic vs. antiperiodic boundary conditions along x are easily implemented by choosing integer or half-integer crystal momenta k . Furthermore, a brief reflection reveals that taking $\Delta_{s1} \Delta_{s2} > 0 (< 0)$ corresponds to periodic (antiperiodic) boundary conditions along y . This is because to complete a full cycle along y an electron must traverse each edge once. When $\Delta_{s1} \Delta_{s2} > 0$ the total phase acquired is 0 or 2π while for $\Delta_{s1} \Delta_{s2} < 0$ it is $\pm\pi$, the latter corresponding to antiperiodic b.c.

To demonstrate the electronic equivalence between the strip and the torus we numerically evaluate the ground state energy E_g of the strip in the four flux sectors as well as the corresponding electron number parity P . According to Ref. [43] the later can be calculated from the knowledge of BdG eigenvectors $\phi_{nk} = (u_{nk}, v_{nk})^T$ be-

longing to positive energy eigenvalues E_{nk} . Specifically, for the strip geometry at hand the parity is given by $P = \prod_k P_k$ with

$$P_k = (-1)^{\text{rank}(V_k)} \quad (24)$$

where V_k is a $(2N_y \times 2N_y)$ matrix of column vectors v_{nk} and N_y denotes the width of the strip.

Our results are summarized in Table I. We find four nearly-degenerate ground states corresponding to four sectors labeled by (ν_x, ν_y) . Three of these belong to the even parity subspace and one to the odd parity subspace. In contrast to the chiral p -wave on a torus we find that $(+, -)$ is the odd-parity ground state. This can be understood as follows: An electron traversing the y -cycle of the strip must flip its spin twice. This can be thought of as a 2π rotation in the spin space which entails additional Berry phase π . Hence, effectively, the $(+, -)$ sector provides periodic boundary conditions along both cycles and hosts the lone odd-parity ground state.

We quantify the ground state degeneracy by parameter $\varepsilon^{(\nu_x, \nu_y)}$ defined as the relative fractional energy difference between $E_g^{(\nu_x, \nu_y)}$ and the average of the four ground state energies E_g^{avg} ,

$$\varepsilon^{(\nu_x, \nu_y)} = \left(E_g^{(\nu_x, \nu_y)} - E_g^{\text{avg}} \right) / |E_g^{\text{avg}}|. \quad (25)$$

For $N_x = 64$ and any $N_y \geq 32$ the two pairs of ground states with the same ν_x are found to be exactly degenerate within our numerical accuracy $\sim 10^{-12}$. The fractional energy splitting between these two pairs is at a $\sim 10^{-10}$ level and is furthermore seen to be decreasing in proportion to $1/N_y$. We thus conclude that the four ground states are indeed exactly degenerate in the thermodynamic limit and obey the 3:1 parity rule characteristic of the chiral p -wave superconductor on a torus.

In the presence of Rashba SOC the bulk $\mathbb{Z}_2^\uparrow \times \mathbb{Z}_2^\downarrow$ symmetry breaks down to a single \mathbb{Z}_2 global parity conservation. Physically, SOC enables Cooper pairs to ‘tunnel’ between spin-up and spin-down sectors of the theory away from the edges of the strip. One thus expects non-zero λ_R to weaken the strip-torus correspondence indicated in Fig. 5 and lift the exact degeneracy between the four ground states. Fig. 6 quantifies this splitting. We observe that increasing λ_R indeed splits the ground-state manifold into two nearly degenerate pairs of states labeled by common ν_y . The split between

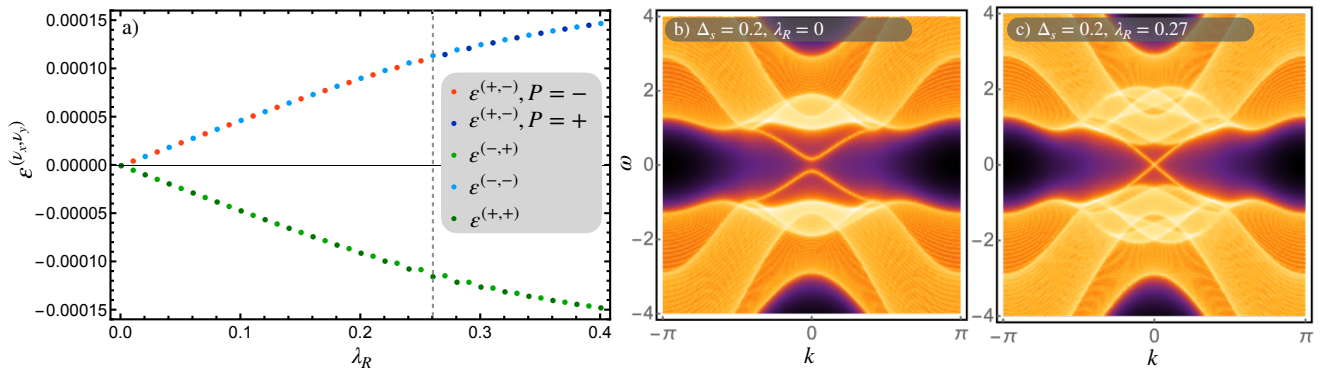


FIG. 6. Splitting of the ground-state degeneracy in the presence of Rashba SOC. Panel (a) shows the fractional energy splitting $\varepsilon^{(\nu_x, \nu_y)}$ as a function of λ_R . The vertical dashed line indicates the transition between even and odd parity of the $(+, -)$ state. Panels (b,c) display edge spectral function $A(\omega, k)$ for $\lambda_R = 0.0$ and 0.27 , the latter marking the closing of the edge energy gap. The same parameters are used as in Table I with $(N_x, N_y) = (64, 32)$.

$\nu_y = +$ and $-$ states grows approximately linearly with λ_R but remains at least two orders of magnitude below all other energy scales (e.g. the bulk excitation gap). For $\lambda_R < \lambda_{Rc} \simeq 0.27$ the system also continues to obey the 3:1 parity rule; for larger λ_R all four ground states belong to the even parity subspace. As shown in panels (b,c) this transition is accompanied by closing of the edge gap. When the gap reopens for larger λ_R the system on the strip can no longer be thought of as topologically equivalent to the torus.

The above behavior can be understood as follows. We know that either Δ_s or Rashba SOC open a gap in the helical edge modes. When both are present the two gaps compete. For $\lambda_R \lesssim \Delta_s$ the edge gap is dominated by the pairing term which we rely on to implement periodic vs. antiperiodic boundary conditions in the y -direction. In this regime the system is sensitive to the sign of $\Delta_{s1}\Delta_{s2}$ and behaves, effectively, as a chiral p -wave SC on a torus. In the opposite regime the edge gap is dominated by SOC which imposes periodic b.c. along y , independent of $\text{sgn}(\Delta_{s1}\Delta_{s2})$. We checked that modifying the Rashba SOC such that λ_R changes sign between the two edges restores the 3:1 parity behavior in this regime. However, it is not clear how this could be implemented experimentally.

We conclude that the ground state degeneracy characteristic of chiral p -wave SC on a torus can indeed be realized in the helical $p_{-}^{\uparrow} \otimes p_{+}^{\downarrow}$ phase of the model placed on the long strip, provided that Rashba SOC is small compared to the SC gap at the edges.

B. Annulus geometry

To study the model in the annulus geometry we write Hamiltonian Eq. (3) in real space and numerically diagonalize the resulting BdG matrix to find its eigenvalues and eigenstates. Fig. 7(a) shows a square lattice cluster that we use to approximate an annulus with inner ra-

dius R_1 , outer radius R_2 and the total number of sites $\sim \pi(R_2^2 - R_1^2)$. Similar to the strip we use SC edge term Eq. (6) (adapted for real-space formulation) to gap out the helical edge modes and take $\Delta^{\text{edge}} = \Delta_{s1} (\Delta_{s2})$ for the inner (outer) edge, with $\text{sgn}(\Delta_{s1}\Delta_{s2})$ controlling the boundary conditions in the radial direction. Antiperiodic b.c. in the polar direction is achieved by inserting a magnetic flux Φ_0 in the hole, accompanied by 2π winding in the SC phase. As explained in Sec. III this is implemented by attaching a minus sign to all tunneling and pairing amplitudes on bonds that cross the positive x axis, green line in Fig. 7(a). The four possible boundary conditions are labeled by a pair of radial and polar indices (ν_r, ν_φ) that are analogous to (ν_x, ν_y) employed in the long strip geometry.

As shown in Fig. 7(b,c) the spectrum of excitations contains gapless edge modes when $\Delta_{sj} = 0$. Taking non-zero Δ_{sj} produces a gap in the edge mode spectrum. In this regime we expect the annulus to behave effectively as a torus. This is indeed confirmed by observing four-fold ground state degeneracy which obeys the characteristic 3:1 parity rule, summarized in Table II. We show results for a clean system described by Eqs. (3) and (6) and in the presence of on-site disorder. This is implemented by adding

$$\mathcal{H}_{\text{dis}} = \sum_{\mathbf{r}, \sigma} \zeta_{\mathbf{r}} c_{\mathbf{r}\sigma}^{\dagger} c_{\mathbf{r}\sigma} \quad (26)$$

to the normal-state Hamiltonian, where \mathbf{r} labels the lattice sites and $\zeta_{\mathbf{r}}$ is a random variable drawn from a uniform distribution between $(-w, w)$. We observe that the fractional energy splitting ε of the ground-state manifold is small ($\sim 10^{-9}$, just above our numerical precision) and is essentially independent of the magnitude of the on-site disorder w . This remains true even for strong disorder with $w = 0.4$, comparable to the bulk SC gap. We conclude that the pattern of the ground-state degeneracy expected of a chiral p -wave SC on a torus is robustly present on the annulus.

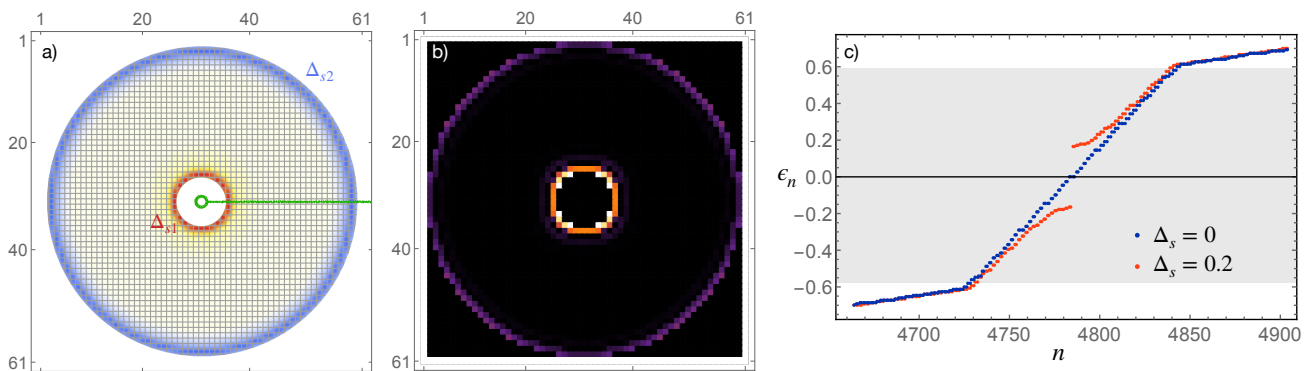


FIG. 7. The $p_-^\uparrow \otimes p_+^\downarrow$ state on an annulus. a) Square lattice cluster containing 2392 sites used to model an annulus with inner radius $R_1 = 5$ and outer radius $R = 28$. Bonds crossing the vertical green line have their hopping and pairing amplitudes reversed when implementing antiperiodic b.c. in the polar direction. b) Wave function amplitude for the lowest positive energy state in the $(-, -)$ sector for $\Delta_{sj} = 0$. The same parameters are used as in Table I. c) Energy eigenvalues of the BdG Hamiltonian plotted against their index n for $\Delta_s = 0$ (blue) and $\Delta_s = 0.2$ (red). Shaded area corresponds to the bulk SC gap. The in-gap states are localized near the edges.

TABLE II. Parity P and the relative ground state energy $\varepsilon^{(\nu_r, \nu_\varphi)} = (E_g^{(\nu_r, \nu_\varphi)} - E_g^{\text{avg}})/|E_g^{\text{avg}}|$ for the four ground state sectors in the annulus geometry described in Fig. 7, as a function of increasing on-site disorder w . The parity is computed from $P = (-1)^{\text{rank}(V)}$ where V is a matrix composed of v_n components of the BdG eigenstate $\phi_n = (u_n, v_n)^T$ belonging to positive eigenvalues E_n . The displayed values of ε reflect a single disorder realization; however, we find very little variation between different realizations indicating that for this size the system is already in the self-averaging regime.

(ν_r, ν_φ)	$(+, +)$	$(+, -)$	$(-, +)$	$(-, -)$
P	+	+	+	-
$\varepsilon(w = 0.0)$	4.09442×10^{-9}	-3.72549×10^{-9}	3.72549×10^{-9}	-4.0944×10^{-9}
$\varepsilon(w = 0.2)$	3.94771×10^{-9}	-3.56987×10^{-9}	3.56987×10^{-9}	-3.94771×10^{-9}
$\varepsilon(w = 0.4)$	3.49598×10^{-9}	-3.09333×10^{-9}	3.09333×10^{-9}	-3.49598×10^{-9}

Table II indicates that on annulus the ground state belonging to the odd parity sector is $(-, -)$. Intuitively, this can be understood as follows. In the radial direction we have the same effect as on the long strip: to complete the cycle electron has to flip spin twice which adds a π Berry phase. In the polar direction there is a difference between the strip and the annulus rooted in distinct trajectories along the respective cycle. On the strip the trajectory is a straight line whereas on the annulus it is a loop encircling the hole. In a $p_x \pm ip_y$ superconductor a Cooper pair acquires a $\pm 2\pi$ Berry phase on completing such a planar loop. This can be seen by thinking about the pair as living on a bond between two sites. Under chiral p -wave pairing these bond fields have non-zero relative phases which add up to $\pm 2\pi$ along any closed, non-intersecting path. A 2π phase for a Cooper pair corresponds to a π phase for an electron – hence, electrons circling a hole experience effectively antiperiodic boundary conditions. As a result we expect the $(\nu_r, \nu_\varphi) = (-, -)$ sector to provide effectively periodic b.c. on the annulus and hence host the odd-parity ground state.

We finally consider the effect of Rashba SOC. Similar to the long strip geometry we expect λ_R to split the ground-state manifold and eventually remove the 3:1 par-

ity pattern characteristic of the chiral p -wave SC on the torus. Fig. 8 shows the splitting quantified by $\varepsilon^{(\nu_r, \nu_\varphi)}$ as calculated for the annulus with 2392 sites. Rashba SOC is seen to split the manifold into two nearly-degenerate sectors labeled by the common ν_r . For small $\lambda_R \lesssim 0.2$ the splitting remains negligible compared to the excitation gap, the 3:1 parity rule is obeyed and the system on annulus can be regarded as equivalent to the chiral p -wave SC on torus. At $\lambda_{Rc} \simeq 0.45$ the edge gap closes marking the transition to a phase dominated by SOC where all four states belong to the even parity sector. The system can no longer be thought of as equivalent to the torus in this regime.

V. DISCUSSION

A. Summary of results

A 2D quantum system whose spin-up electrons possess topological order TO while spin-down electrons possess its time-reversal conjugate, forming together a combined $\text{TO} \otimes \bar{\text{TO}}$ state, exhibits ground-state topological degeneracy characteristic of the TO on the torus when placed

on an annulus with symmetry-breaking edges. Such an annular geometry is generically much better suited for experimental investigations than torus. Our results based on a simple microscopic model can be viewed as providing microscopic grounding for the ideas introduced recently in Ref. [16] in the context of twisted homobilayer MoTe₂ which may support $\text{Pf}^\uparrow \otimes \overline{\text{Pf}}^\downarrow$ topological order according to the recent experimental report [17].

Alternately, our model is applicable directly to superconducting altermagnets where it provides a blueprint for probing topological degeneracy in a new family of materials. The key theoretical insight is that characteristic spin-split fermi surfaces of altermagnets are naturally suited for the emergence of chiral p -wave superconductivity which is the leading instability in the presence of weak attractive interactions [39, 40]. This is a direct consequence of the fact that, as illustrated in Fig. 2(a), one must pair same-spin electrons to form a Cooper pair. For this reason, one generically expects metallic altermagnets to exhibit odd-parity SC order when cooled to sufficiently low temperatures.

In the strict non-relativistic limit (i.e. vanishing Rashba SOC) the Hamiltonian describing such SC altermagnet remains diagonal in spin space and obeys the $\mathbb{Z}_2^\uparrow \times \mathbb{Z}_2^\downarrow$ spin conservation. This leads to 4 possible ground states with either p_+ or p_- orbital pair wave-function for each spin projection. In the presence of weak Rashba SOC or spin-singlet SC order spontaneously generated near the edges, the $p_-^\uparrow \otimes p_+^\downarrow$ helical state becomes energetically favored, furnishing a concrete realization of the $\text{TO} \otimes \overline{\text{TO}}$ state. We established the ground state degeneracy of this state in long strip and annular geometries by an explicit numerical diagonalization of the relevant Bogoliubov-de Gennes Hamiltonians. The observed degeneracy becomes exact in the thermodynamic limit, shows the 3:1 parity pattern expected for the chiral p -wave SC on the torus and is robust with respect to disorder.

When Rashba SOC is present in the system the protecting $\mathbb{Z}_2^\uparrow \times \mathbb{Z}_2^\downarrow$ symmetry is broken down to the global \mathbb{Z}_2 parity conservation. The ground state degeneracy is then split in proportion to the SOC strength λ_R . For λ_R small compared to the excitation gap the 3:1 parity rule continues to hold and the system can still be thought of as living effectively on an ‘imperfect’ or ‘fuzzy’ torus with a weak tunneling between its opposite walls enabled via SOC. We thus find that, perhaps not surprisingly, the topological equivalence between torus and annulus indicated in Fig. 1 is exact only when the bulk of the system respects the protecting symmetry. This, however, will be true for any TO, including the putative $\text{Pf}^\uparrow \otimes \overline{\text{Pf}}^\downarrow$ phase in MoTe₂. On the annulus, because TO and $\overline{\text{TO}}$ are overlapping in real space, the topological order becomes symmetry-protected.

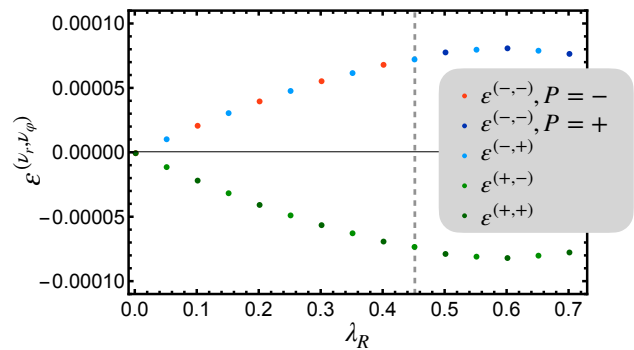


FIG. 8. Splitting of the ground-state degeneracy on the annulus in the presence of Rashba SOC. Vertical dashed line marks the transition in parity P of the $(-, -)$ ground state. The same parameters as used as in Table II with $w = 0$. Including on-site disorder does not significantly change these results.

B. Experimental connections

If twisted bilayer MoTe₂ indeed harbor the $\text{Pf}^\uparrow \otimes \overline{\text{Pf}}^\downarrow$ phase then annulus-shaped samples could be used to probe the corresponding ground-state degeneracy as discussed in Ref. [16]. Conversely, such measurements could be used to shed light on the nature of the TO in this material in ways that are complementary to the edge-mode conduction results reported in Ref. [17]. Below we discuss how this physics would manifest in altermagnet realization of $\text{TO} \otimes \overline{\text{TO}}$.

Although no material realizations of SC altermagnets have been reported to date, many altermagnet candidates have recently been identified [33–38] and the characteristic spin-split electron bands have already been experimentally observed in some of them [27–30]. Since many of these materials are good metals one expects superconductivity to occur in some of them at sufficiently low temperatures. Importantly, the propensity of altermagnets to form odd-parity SC order is encoded in their normal-state band structure and does not require any unusual form of electron-electron interaction; the ubiquitous phonon mediated attraction is perfectly adequate. Also, because the magnetism is compensated, it will not interfere with the onset of superconducting order.

Assuming a suitable SC altermagnet becomes available in the near future, how can we use it to experimentally probe the ground-state degeneracy phenomena discussed in this paper? Before we attempt to answer this question it is necessary to highlight an important distinction between the ground state degeneracy in FQH liquids and superconductors. While degeneracy in both systems is associated with fluxes threading torus holes, in FQH the gauge field is emergent and as such exists only within the material itself. The degeneracy is intrinsic in that the relevant many-body Hamiltonian fully captures the gauge field dynamics, and, when diagonalized, exhibits the requisite number of degenerate ground states in its

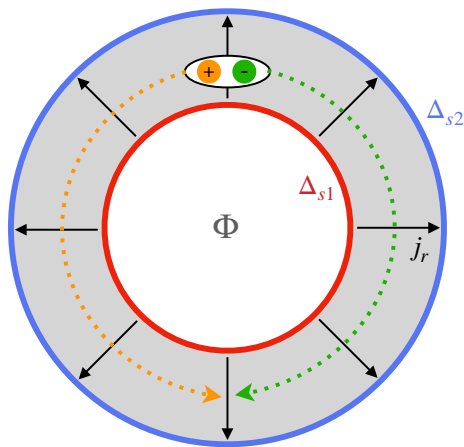


FIG. 9. Schematic setup for probing the ground state degeneracy in the $p^\uparrow \otimes p^\downarrow$ superconducting ring. Magnetic flux Φ is used to control index ν_φ while the radial current density j_r can be applied to promote vortex/antivortex unbinding and recombination. As explained in the text such events switch between the two ν_r sectors.

spectrum. In superconductors, by contrast, the degeneracy is associated with the real electromagnetic field which exists outside the material and enters the BdG Hamiltonian as an external parameter, see e.g. Eq. (15). It would become a true degeneracy if the EM field were treated as dynamical. However, we know that at energy and length scales that are at play in solid-state systems quantum fluctuations of the magnetic flux through the SC ring are negligible. Hence, the toroidal ground state degeneracy in a superconductor is best regarded as a statement of energetic equivalence between states containing even vs. odd number of SC flux quanta.

When viewed in this light the classic Little-Parks flux quantization experiment [44, 45] can be regarded as experimental confirmation of sorts of the expected energetic equivalence in conventional spin-singlet superconductors. The question then arises: Can we use the torus/annulus equivalence to go further and probe the degeneracy specific to the chiral p -wave superconductor? In practice this would entail testing the 3:1 parity rule that distinguishes the chiral p -wave state. In the remainder of this subsection we outline possible strategies to achieve this.

At a minimum, to probe the topological degeneracy, one needs a way to switch between the energy minima controlled by the boundary conditions labeled by the pair of indices (ν_r, ν_φ) . Inspection of Fig. 7(a) and Table II suggests the following approach. The ν_φ index can be controlled straightforwardly by adjusting the applied magnetic field B perpendicular to the plane of the annulus. For practical reasons it is best to employ a ring geometry with a large hole (i.e. R_1 only slightly smaller than R_2) such that the flux $\Phi_0 = \pi R_1^2 B$ through the hole corresponds to a sufficiently weak field permeating the superconductor as can be neglected. Then one could switch between the two ν_φ sectors by simply changing

the applied field.

The two ν_r sectors are controlled by the relative sign of Δ_{s1} and Δ_{s2} . Switching between them can be achieved by nucleating a vortex-antivortex pair in one spin sector, dragging its constituents around the hole as indicated in Fig. 9, and then annihilating the pair. Vortex-antivortex pairs occur naturally as quantum or thermal fluctuations in a 2D superconductor. Deep in the SC phase such pairs are bound and the probability of a pair dissociating and recombining after its constituents have travelled along the opposite branches of the annulus is negligible. Imagine, however, that we attach electrical contacts to the inner and outer edges of the annulus and drive current J_r between them. Ideally, the current density will be uniform around the ring with the current flowing in the radial direction as indicated in Fig. 9, but this is not essential. In the presence of the radial current the members of a spontaneously nucleated vortex-antivortex pair will feel Magnus force that is perpendicular to the current direction and opposite for the vortex and the antivortex. For a sufficiently large applied current one expects the probability of the above encircling process to become significant. In essence, the applied current will tear apart a vortex-antivortex pair that has become sufficiently large such that the Magnus force overcomes their attraction. It will also assist their journey around the hole. Importantly, such a process is analogous to a phase slip which advances the phase difference between the inner and the outer edge by 2π . If a single such event occurs in one spin species, the net effect dictated by Eq. (23) is precisely to change the relative sign between Δ_{s1} and Δ_{s2} .

We conclude that, at least in principle, it is possible to switch between the 4 ground state sectors of the annulus by adjusting the applied magnetic field B and the radial current J_r , as discussed above. Now suppose we perform a Little-Parks type experiment by increasing J_r close to its critical value. In this regime the resistance will be dominated by phase slips and we can think of the annulus as flipping between $\nu_r = \pm$ sectors. According to Table II, for zero flux Φ through the hole (corresponding to the $\nu_\varphi = +$ sector), both ν_r ground states belong to the same even parity subspace. For $\Phi = \Phi_0$, the system will be in the $\nu_\varphi = -$ sector. In this case, flipping ν_r will cause the system to switch between even and odd parity ground states. If the ring is electronically isolated such that the parity P is conserved then switching from the $(-, +)$ sector to $(-, -)$ will drive the system to an excited state, with one fermionic quasiparticle above the odd-parity ground state. Hence, one would expect to see an energetic difference in Little-Parks oscillations between zero-flux and $\Phi = \Phi_0$ cases. If the parity is not conserved then there will be no energy difference; in this case one could employ a direct parity detection scheme [46, 47] to identify the $\nu_\varphi = \pm$ sectors.

C. Outlook

Theoretical developments in Ref. [16] and in this work suggest that topological degeneracy, first conceptualized in works of Haldane, Wen and others more than 30 years ago [1–3], could be experimentally tested in a class of systems that support two copies of time-reversed topological order $\text{TO} \otimes \overline{\text{TO}}$. In this study we performed a detailed analysis of a specific example furnished by a $p_{-}^{\uparrow} \otimes p_{+}^{\downarrow}$ superconducting phase that we expect to naturally form in metallic altermagnets at sufficiently low temperatures. By virtue of the Read-Green correspondence [21] this phase shares key topological properties with the $\text{Pf}^{\uparrow} \otimes \overline{\text{Pf}}^{\downarrow}$ fractional quantum Hall liquid that may be realized in twisted homobilayers of MoTe_2 . The chief advantage of considering the $p_{-}^{\uparrow} \otimes p_{+}^{\downarrow}$ superconducting example lies in its tractability: a treatment at the level of the conventional mean-field BCS theory allowed us to explicitly evaluate ground state energies, the corresponding parity eigenvalues, and confirm in detail the expected ground state degeneracies for various sample geometries, including the experimentally accessible annulus.

Our main conclusion based on these results is that a SC altermagnet fabricated in a ring geometry Fig. 7(a) could indeed be used to probe the topological degeneracy. A key requirement is that the material respects the $\mathbb{Z}_2^{\uparrow} \times \mathbb{Z}_2^{\downarrow}$ spin-conservation symmetry in the bulk (i.e. away from the edges). In practice this means negligible Rashba SOC as well as any perturbations that flip electron spin, such as magnetic impurities. We showed that ground state degeneracy is robust to non-magnetic disorder but spin-flip inducing perturbations are detrimental in that they split the degeneracy in proportion to their strength. Nevertheless, some key signatures, such as the characteristic 3:1 parity property, persist up to a critical strength of spin-flip perturbations. We note that this requirement is generic and applies to any $\text{TO} \otimes \overline{\text{TO}}$.

We conclude by listing possible broader impacts of this work. A ring with $p_{-}^{\uparrow} \otimes p_{+}^{\downarrow}$ superconducting order depicted in Fig. 7(a) could be used as a protected qubit. We envision the two logical states encoded as two ground states labeled by $\nu_r = \pm$ with fixed ν_{φ} set by the external magnetic flux Φ . The qubit is protected because the information is encoded *non-locally* in $\text{sgn}(\Delta_{s1}\Delta_{s2})$ and measuring one Δ_{sj} alone does not provide any information on the state. Instead, to read out the qubit, one must perform a measurement of the relative phase between Δ_{s1} and Δ_{s2} and this is necessarily a non-local measurement given that inner and outer edges are macroscopically separated. In the $\nu_{\varphi} = -$ sector the product $\text{sgn}(\Delta_{s1}\Delta_{s2})$ encodes the ring electron parity P , in a way reminiscent of two Majorana zero modes localized e.g. at the ends of a quantum wire. In the present case, however, the underlying system is fully gapped and hence, presumably, more robustly immune to decoherence.

Another important realization is the fact that metal-

lic altermagnets are generically expected to harbor odd-parity superconducting orders, with chiral p -wave being the most natural in the square lattice and f -wave in hexagonal crystals. This has been first noted in Ref. [39] and our work [40] confirms this expectation. Such an exotic superconductivity has been long sought by the materials community but never convincingly demonstrated in any material to date. Another logical possibility, not considered in this paper, is spin-singlet pairing at non-zero Cooper pair momentum (the Fulde-Ferrel-Larkin-Ovchinnikov type state) discussed in Ref. [48]. Such a state is also exotic and rare, especially in zero applied magnetic field. Hence, comprehensive search for superconducting instabilities in metallic altermagnets constitutes a promising direction for future research, likely to yield exciting discoveries.

ACKNOWLEDGMENTS

We are grateful to Ching-Kai Chiu, Niclas Heinsdorf, Masaki Oshikawa, Adarsh Patri, Andrew Potter, Nicholas Read, Rui Wen and Ashvin Vishwanath for illuminating discussions and correspondence. This research was supported in part by NSERC, CIFAR, and the Canada First Research Excellence Fund, Quantum Materials and Future Technologies Program.

Appendix A: Effect of Rashba SOC and spin-singlet SC

We wish to understand the effect of adding a weak Rashba SOC or a spin-singlet SC order parameter component on 4 degenerate ground states discussed in Sec. IIB. The former arises generically when a sample is placed on a substrate which breaks the inversion symmetry of the model. The latter can then arise spontaneously from attractive interactions in the sample or can be induced externally by a proximity effect with a conventional spin-singlet superconductor.

To study the energetics of the model in the presence of these perturbation we compute the many-body ground state energy given for the Hamiltonian Eq. (3) as

$$E_g(\varphi) = - \sum_{\mathbf{k}} E_{\mathbf{k}\mu}(\varphi), \quad (\text{A1})$$

where $E_{\mathbf{k}\mu}$ are the positive eigenvalues of the BdG matrix $H_{\mathbf{k}}$. This energy will depend on the relative phase φ of the two SC order parameters which are uncoupled in the unperturbed system. Specifically, we assume $\Delta_{\uparrow} = \Delta_p$ and $\Delta_{\downarrow} = e^{i\varphi} \Delta_p$ with Δ_p real positive.

The result in the presence of Rashba SOC is given in Fig. 10(a). It shows that nonzero λ_R favors the helical $p_{-}^{\uparrow} \otimes p_{+}^{\downarrow}$ state and the absolute minimum occurs at $\varphi = 0$.

To study the effect of spin-singlet SC component we generalize the pair-field matrix entering the BdG Hamil-

tonian as follows,

$$\hat{\Delta}_{\mathbf{k}} = \begin{pmatrix} \Delta_{\mathbf{k}\uparrow} & \Delta_s \\ \Delta_s & \Delta_{\mathbf{k}\downarrow} \end{pmatrix}, \quad (\text{A2})$$

where Δ_s is the spin-singlet amplitude. The resulting ground state energy is shown in Fig. 10(b). Once again the absolute minimum occurs at $\varphi = 0$ but in this case the two helical states remain degenerate while the chiral states are pushed to higher energy.

Panel (c) finally shows the effect of in-plane applied magnetic field B_x . This has the opposite effect to the two \mathcal{T} -respecting perturbations and selects the two chiral phases as ground states.

We thus conclude that both \mathcal{T} -respecting perturbations favor the helical states in accord with the intuitive reasoning presented in the main text and with Ref. [39]. When both Rashba SOC and with non-zero Δ_s are present, there is a single non-degenerate ground state characterized as $p_{-}^{\uparrow} \otimes p_{+}^{\downarrow}$.

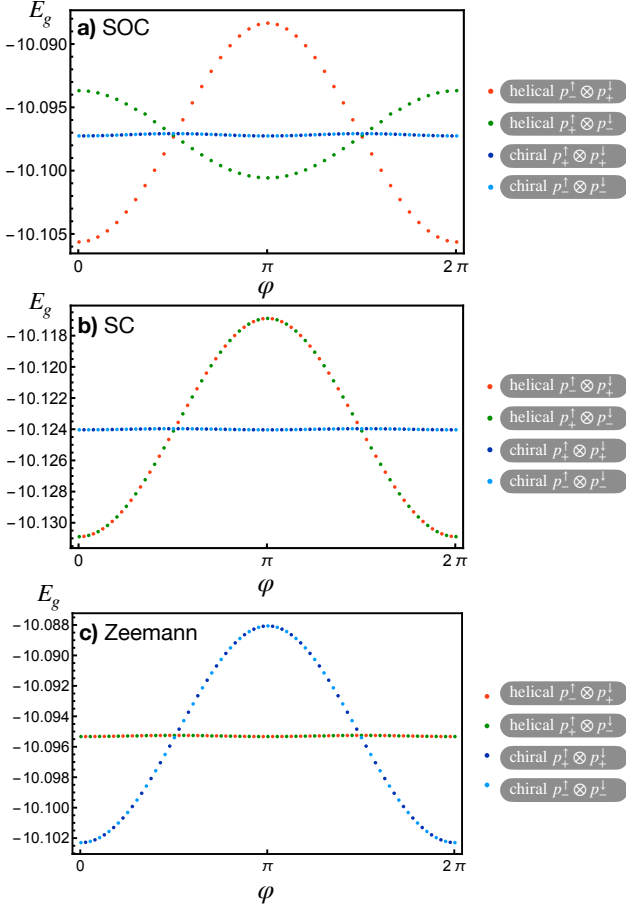


FIG. 10. Ground state energy as a function of the relative phase φ in the presence of (a) Rashba SOC, (b) spin-singlet SC order parameter and (c) in-plane external magnetic field B_x . We use $\eta = 0.2$, $\mu = -2.1$, $\Delta_{\sigma} = 0.5$ and $(\lambda_R, \Delta_s, B_x) = (0.1, 0.0, 0.0)$ in (a) $(0.0, 0.2, 0.0)$ in (b) and $(0.0, 0.0, 0.2)$ in (c).

- [1] F. D. M. Haldane and E. H. Rezayi, *Phys. Rev. B* **31**, 2529 (1985).
- [2] X. G. Wen and Q. Niu, *Phys. Rev. B* **41**, 9377 (1990).
- [3] X.-G. Wen, *International Journal of Modern Physics B* **05**, 1641 (1991).
- [4] J. Nakamura, S. Liang, G. C. Gardner, and M. J. Manfra, *Nature Physics* **16**, 931 (2020).
- [5] H. K. Kundu, S. Biswas, N. Ofek, V. Umansky, and M. Heiblum, *Nature Physics* **19**, 515 (2023).
- [6] J. Leinaas and J. Myrheim, *Il nuovo cimento* **37**, 132 (1977).
- [7] F. Wilczek, *Physical review letters* **49**, 957 (1982).
- [8] X. G. Wen, *Phys. Rev. Lett.* **66**, 802 (1991).
- [9] M. Greiter and F. Wilczek, *Annual Review of Condensed Matter Physics* **15**, 131 (2024).
- [10] E. Verlinde, *Nuclear Physics B* **300**, 360 (1988).
- [11] T. Einarsson, *Phys. Rev. Lett.* **64**, 1995 (1990).
- [12] M. Oshikawa and T. Senthil, *Phys. Rev. Lett.* **96**, 060601 (2006).
- [13] M. Oshikawa, Y. B. Kim, K. Shtengel, C. Nayak, and S. Tewari, *Annals of Physics* **322**, 1477 (2007).
- [14] A. Kitaev, *Annals of Physics* **303**, 2 (2003).
- [15] C. Nayak, S. H. Simon, A. Stern, M. Freedman, and S. Das Sarma, *Rev. Mod. Phys.* **80**, 1083 (2008).
- [16] R. Wen and A. C. Potter, “Cheshire qudits from fractional quantum spin hall states in twisted mote₂,” (2024), [arXiv:2407.03401 \[cond-mat.str-el\]](https://arxiv.org/abs/2407.03401).
- [17] K. Kang, B. Shen, Y. Qiu, Y. Zeng, Z. Xia, K. Watanabe, T. Taniguchi, J. Shan, and K. F. Mak, *Nature* **628**, 522 (2024).
- [18] G. Moore and N. Read, *Nuclear Physics B* **360**, 362 (1991).
- [19] A. P. Reddy, N. Paul, A. Abouelkomsan, and L. Fu, *Phys. Rev. Lett.* **133**, 166503 (2024).
- [20] C.-E. Ahn, W. Lee, K. Yananose, Y. Kim, and G. Y. Cho, *Phys. Rev. B* **110**, L161109 (2024).
- [21] N. Read and D. Green, *Phys. Rev. B* **61**, 10267 (2000).
- [22] S. Hayami, Y. Yanagi, and H. Kusunose, *Journal of the Physical Society of Japan* **88**, 123702 (2019).
- [23] L. Šmejkal, J. Sinova, and T. Jungwirth, *Phys. Rev. X* **12**, 031042 (2022).
- [24] L. Šmejkal, J. Sinova, and T. Jungwirth, *Phys. Rev. X* **12**, 040501 (2022).
- [25] I. Mazin (The PRX Editors), *Phys. Rev. X* **12**, 040002 (2022).
- [26] Y.-P. Zhu, X. Chen, X.-R. Liu, Y. Liu, P. Liu, H. Zha, G. Qu, C. Hong, J. Li, Z. Jiang, X.-M. Ma, Y.-J. Hao, M.-Y. Zhu, W. Liu, M. Zeng, S. Jayaram, M. Lenger, J. Ding, S. Mo, K. Tanaka, M. Arita, Z. Liu, M. Ye, D. Shen, J. Wrachtrup, Y. Huang, R.-H. He, S. Qiao, Q. Liu, and C. Liu, *Nature* **626**, 523 (2024).
- [27] J. Krempaský, L. Šmejkal, S. W. D’Souza, M. Hájlaoui, G. Springholz, K. Uhlířová, F. Alarab, P. C. Constantinou, V. Strocov, D. Usanov, W. R. Pudelpko, R. González-Hernández, A. Birk Hellenes, Z. Jansa, H. Reichlová, Z. Šobáň, R. D. Gonzalez Betancourt, P. Wadley, J. Sinova, D. Kriegner, J. Minár, J. H. Dil, and T. Jungwirth, *Nature* **626**, 517 (2024).
- [28] S. Lee, S. Lee, S. Jung, J. Jung, D. Kim, Y. Lee, B. Seok, J. Kim, B. G. Park, L. Šmejkal, C.-J. Kang, and C. Kim, *Phys. Rev. Lett.* **132**, 036702 (2024).
- [29] O. Fedchenko, J. Minár, A. Akashdeep, S. W. D’Souza, D. Vasilyev, O. Tkach, L. Odenbreit, Q. Nguyen, D. Kutnyakhov, N. Wind, L. Wenthhaus, M. Scholz, K. Rossnagel, M. Hoesch, M. Aeschlimann, B. Stadtmüller, M. Kläui, G. Schönhense, T. Jungwirth, A. B. Hellenes, G. Jakob, L. Šmejkal, J. Sinova, and H.-J. Elmers, *Science Advances* **10**, eadj4883 (2024).
- [30] S. Reimers, L. Odenbreit, L. Šmejkal, V. N. Strocov, P. Constantinou, A. B. Hellenes, R. Jaeschke Ubierno, W. H. Campos, V. K. Bharadwaj, A. Chakraborty, T. Denneulin, W. Shi, R. E. Dunin-Borkowski, S. Das, M. Kläui, J. Sinova, and M. Jourdan, *Nature Communications* **15**, 2116 (2024).
- [31] D. A. Ivanov, *Phys. Rev. Lett.* **86**, 268 (2001).
- [32] T. Hansson, V. Oganessian, and S. Sondhi, *Annals of Physics* **313**, 497 (2004).
- [33] M. Naka, S. Hayami, H. Kusunose, Y. Yanagi, Y. Motome, and H. Seo, *Nature Communications* **10**, 4305 (2019).
- [34] L.-D. Yuan, Z. Wang, J.-W. Luo, E. I. Rashba, and A. Zunger, *Phys. Rev. B* **102**, 014422 (2020).
- [35] I. I. Mazin, K. Koepernik, M. D. Johannes, R. González-Hernández, and L. Šmejkal, *Proceedings of the National Academy of Sciences* **118**, e2108924118 (2021).
- [36] S. Bhowal and N. A. Spaldin, “Magnetic octupoles as the order parameter for unconventional antiferromagnetism,” (2022), [arXiv:2212.03756 \[cond-mat.str-el\]](https://arxiv.org/abs/2212.03756).
- [37] Y. Guo, H. Liu, O. Janson, I. C. Fulga, J. van den Brink, and J. I. Facio, *Materials Today Physics* **32**, 100991 (2023).
- [38] I. V. Maznichenko, A. Ernst, D. Maryenko, V. K. Dugaev, E. Y. Sherman, P. Buczek, S. S. P. Parkin, and S. Ostanin, “Fragile altermagnetism and orbital disorder in mott insulator latio₃,” (2024), [arXiv:2411.00583 \[cond-mat.mtrl-sci\]](https://arxiv.org/abs/2411.00583).
- [39] D. Zhu, Z.-Y. Zhuang, Z. Wu, and Z. Yan, *Phys. Rev. B* **108**, 184505 (2023).
- [40] S. T. F. Heung and M. Franz, “Superconducting instabilities of altermagnetic metals,” (2024), [unpublished](#).
- [41] O. Vafeek, A. Melikyan, M. Franz, and Z. Tešanović, *Phys. Rev. B* **63**, 134509 (2001).
- [42] T. Liu and M. Franz, *Phys. Rev. B* **92**, 134519 (2015).
- [43] G. Ben-Shach, A. Haim, I. Appelbaum, Y. Oreg, A. Yacoby, and B. I. Halperin, *Phys. Rev. B* **91**, 045403 (2015).
- [44] R. Doll and M. Näbauer, *Phys. Rev. Lett.* **7**, 51 (1961).
- [45] W. A. Little and R. D. Parks, *Phys. Rev. Lett.* **9**, 9 (1962).
- [46] P. Lafarge, P. Joyez, D. Esteve, C. Urbina, and M. H. Devoret, *Phys. Rev. Lett.* **70**, 994 (1993).
- [47] E. T. Mannila, V. F. Maisi, H. Q. Nguyen, C. M. Marcus, and J. P. Pekola, *Phys. Rev. B* **100**, 020502 (2019).
- [48] D. Chakraborty and A. M. Black-Schaffer, “Zero-field finite-momentum and field-induced superconductivity in altermagnets,” (2024), [arXiv:2309.14427 \[cond-mat.supr-con\]](https://arxiv.org/abs/2309.14427).